Nearly complete stress drop in the 2011 M_w 9.0 off the Pacific coast of Tohoku Earthquake

Akira Hasegawa, Keisuke Yoshida, and Tomomi Okada

Research Center for Prediction of Earthquakes and Volcanic Eruptions, Graduate School of Science, Tohoku University, Sendai 980-8578, Japan

(Received April 25, 2011; Revised June 2, 2011; Accepted June 3, 2011; Online published September 27, 2011)

Temporal change in the stress field after the 2011 Tohoku earthquake was observed by stress tensor inversions of focal mechanisms of earthquakes near the source region. The maximum compressive stress (σ_1) axis before the earthquake has a direction toward the plate convergence, dipping oceanward at an angle of 25–30 degrees. Its dip angle significantly increased by 30–35 degrees after the earthquake, and σ_1 axis came to intersect with the plate interface at a high angle of about 80 degrees. By using the observed rotation of σ_1 axis, we estimated the ratio of mainshock stress drop to the background deviatoric stress $\Delta\tau/\tau$ to be 0.9–0.95. This shows that the deviatoric stress causing the M_w 9.0 earthquake was mostly released by the earthquake, or the stress drop during the earthquake was nearly complete. Adopting the average stress drop obtained by GPS observation data, the deviatoric stress magnitude is estimated to be 21–22 MPa. This suggests the plate interface is weak. The nearly complete stress drop caused a high dip angle of σ_1 axis, which is the reason why not a small number of normal fault type aftershocks have occurred.

Key words: 2011 Tohoku earthquake, NE Japan subduction zone, deviatoric stress magnitude, weak fault.

1. Introduction

It is particularly important for the mitigation of earthquake hazards to understand why such a great earthquake as the 2011 Tohoku earthquake with magnitude 9.0 did occur along the plate boundary east off northeastern Japan, since the occurrence of a M 9 class earthquake there was not predicted in the long-term evaluation of earthquake occurrence in Japan by the Japanese government (Earthquake Research Committee, Headquarters for Earthquake Research Promotion, http://www.jishin.go.jp/main/index-e.html). Stress acting on the plate boundary which caused this earthquake is one of basic information for this purpose. It is important to know how large the shear stress is to cause earthquake rupture and how much portion of that stress is released by it. Of particular interest is whether the shear stress is nearly completely released by such a great earthquake which ruptured a half or two thirds of the entire main thrust zone east of northeastern Japan at once. However, estimation of magnitude of the shear stress acting on faults at depths prior to large earthquakes remains the subject of controversy.

In the present paper, we try to extract information on the deviatoric stress causing the 2011 Tohoku earthquake from earthquake focal mechanism data before and after its occurrence. Figure 1 shows one example of distributions of P and T-axes of earthquake focal mechanisms before and after the 2011 earthquake. The figure clearly shows that most of the events have P-axes dipping oceanward and that the average dip angle became steeper after the 2011 earthquake. This suggests the change of stress field due to the 2011 earthquake, which gives a unique opportunity to estimate deviatoric stress magnitude. We estimate the amount of stress released by the earthquake from the rotation angle of the maximum principal stress (σ_1) axis before and after the earthquake.

2. Data and Method

We used focal mechanism data of earthquakes that occurred near the plate interface in the aftershock area of the 2011 Tohoku earthquake before and after its occurrence. Focal mechanisms used are those determined by moment tensor inversions of F-net data of the National Research Institute for Earth Science and Disaster Prevention (NIED) (http://www.bosai.go.jp/e/index.html). The data period is from 1997 to April 6, 2011, thus including earthquake data both before and after the Tohoku earthquake. Earthquakes with M_w larger than 4.0 and variance reductions better than 70% that occurred within 12.5 km from the plate interface both above and below it are selected. The value of 12.5 km was chosen in order to generate a data set for events near the plate interface. A somewhat different distance, for example, 20 km or so, does not change the results significantly. The geometry of the subducting Pacific plate used is that estimated by Nakajima *et al.* (2009).

Stress tensor inversion analyses were made by using events located in the two rectangle regions (regions A and B in the inset map of Fig. 2), which roughly correspond to the northern and southern halves of the aftershock area. The numbers of focal mechanisms are 246 and 552 in regions A and B, respectively, for the pre-mainshock period. We have

doi:10.5047/eps.2011.06.007

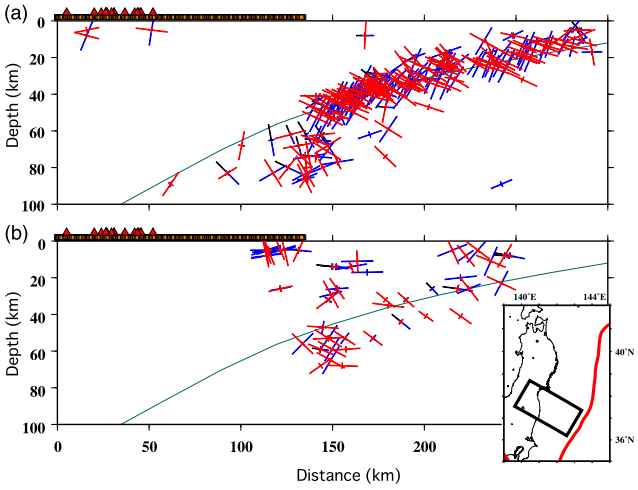

Fig. 1. P and T axis distributions of earthquake focal mechanisms (a) before and (b) after the 2011 Tohoku earthquake projected on a vertical plane perpendicular to the trench axis. P and T axes for earthquakes in the rectangle region in the inset map are plotted. Focal mechanisms are from the seismic moment tensor catalogue by the NIED. P- and T-axes are shown by red and blue lines, respectively. Orange horizontal lines and red triangles on the top show the locations of the land area and active volcanoes, respectively. Inclined lines denote the upper plate boundary.

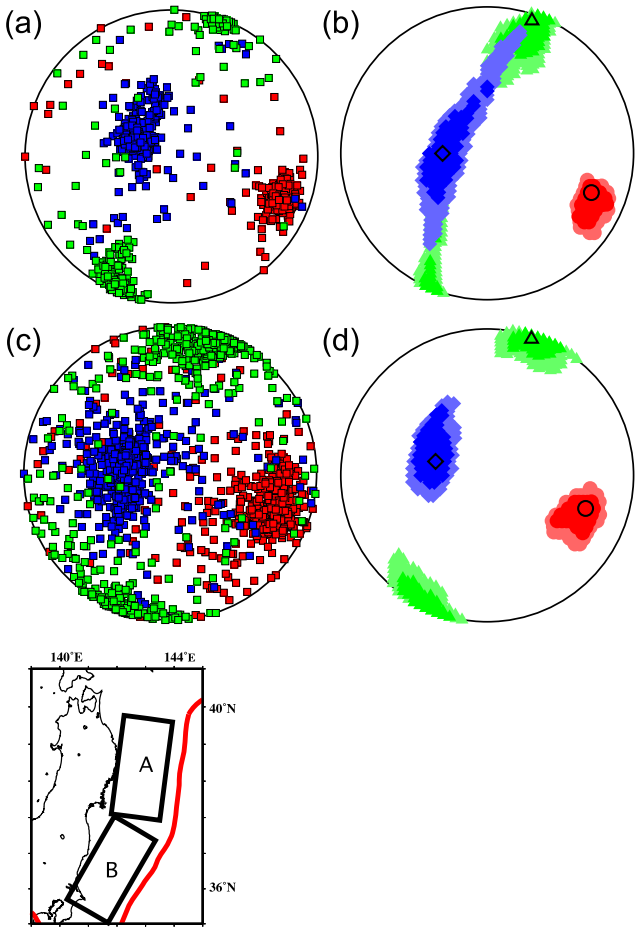

Fig. 2. (a) P (red square), B (green) and T (blue) axes of focal mechanisms and (b) best fit principal stress σ_1 (red circle), σ_2 (green triangle) and σ_3 (blue square) projected on the lower focal hemisphere by equal area projection for earthquakes that occurred before the Tohoku earthquake in region A. (c) and (d) show those for events in region B. In (b) and (d), principal stresses falling within 68% and 95% confidence levels are shown by lighter colors. Focal mechanisms for the period of 1997–March 10 2011 are used for the inversions.

30 and 52 focal mechanisms in regions A and B for the post-mainshock period. P, B and T-axes of focal mechanisms in regions A and B for the pre-mainshock period are shown in Figs. 2(a) and (c). Similarly, those in regions A and B for the post-mainshock period are shown in Figs. 3(a) and (c).

In order to investigate how the stress field may change with time, we invert focal mechanism data during five periods: 1997–March 10 2011, 1997–2004, May 2000–May 2007, 2004–March 10 2011, and March 12 2011–April 6 2011. The former four periods are before the mainshock and the last period is after the mainshock. The computer code of Ito *et al.* (2009) was used for the stress tensor inversions. Like other methods of stress tensor inversions, the code uses a grid search algorithm to search for the minimum summation of the misfit angles of all focal mechanisms in order to obtain the best fit model. The confidence limits for an acceptable range of the best fit model were defined by the method of Gephart and Forsyth (1984). Applying the code to focal mechanism data in regions A and B for each period, we obtain orientation of the principal stresses.

3. Temporal Change of the Stress Field

Stress tensor inversion results for the period before the 2011 Tohoku mainshock are shown for region A in Fig. 2(b) and for B in Fig. 2(d). Similarly, results for the period after the mainshock are shown in Figs. 3(b) and (d). In these stress tensor inversions, we assume that events occur along fault planes having various strikes and dips, and slip occurs in a direction of shear stress on those planes. Thus we consider some events occur on the plate interface but others occur off the plate interface. Comparison of Fig. 2 with Fig. 3 shows a clear change in dip angle of σ_1 axis: both in A and B regions it is about 25–30 degrees during the pre-mainshock period, whereas it increased to about 60 degrees after the mainshock.

Inversion results for the periods of 1997–2004, May 2000–May 2007, and 2004–March 10 2011 give similar orientation of the principal stresses to that for the period of 1997–March 10 2011, though not shown here. All these period data show that the dip angle of σ_1 axis is 25–30 degrees, which suggests that it did not change significantly through the time at least for about the 14-year period before the Tohoku earthquake.

The Pacific plate subducts at a very shallow angle of about 10 degrees for the first 20 km depth or so, and then steepens with a dip angle gradually increasing up to about 30 degrees at ~50 km depth, the downdip end of the source area of the 2011 Tohoku earthquake (Umino *et al.*, 1995). Here we assume the average dip angle of the plate interface to be 20 degrees. Figure 4 shows temporal evolution of the stress field during the period from 1997 to April 6 2011, in which an angle θ between σ_1 axis and the plate interface is shown as a function of time. The figure clearly shows that the intersecting angle θ significantly changed after the mainshock, from 45–50 degrees to a very high angle of

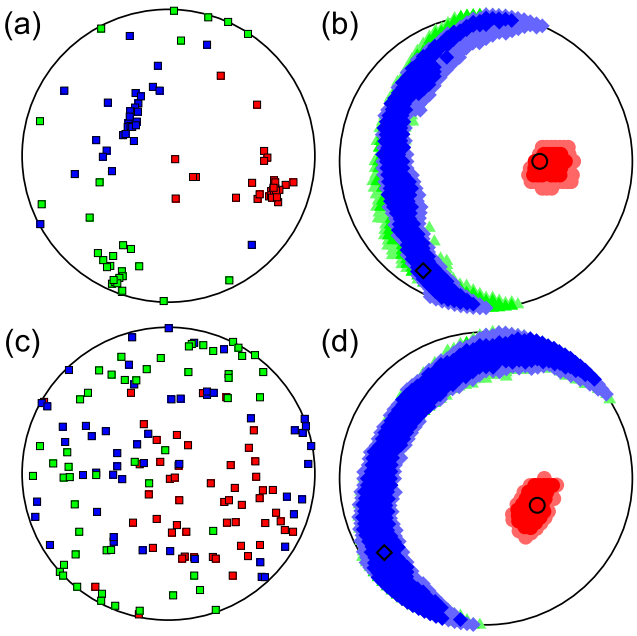

Fig. 3. (a) P, B and T axes of focal mechanisms and (b) best fit principal stress σ_1, σ_2 and σ_3 for earthquakes that occurred after the east off Tohoku earthquake in region A. (c) and (d) show those for events in region B. Focal mechanisms for the period of March 12–April 6 2011 are used for the inversions. Others are the same as in Fig. 2.

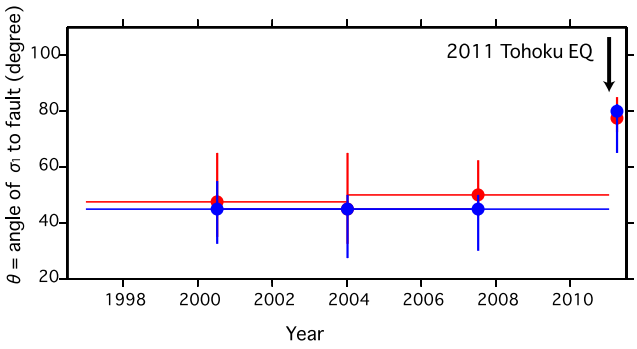

Fig. 4. Temporal change of angle of σ_1 to the mainshock fault plane. Those for regions A and B are shown by red and blue circles, respectively. Vertical lines show the confidence range.

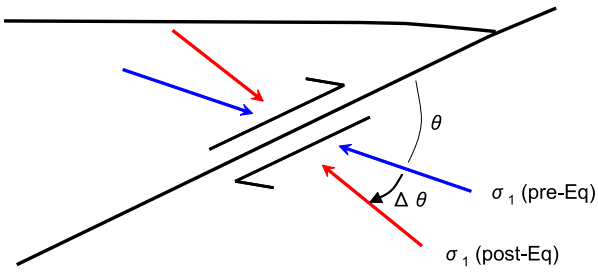

Fig. 5. Assumed geometry of stress rotation due to slip on the fault.

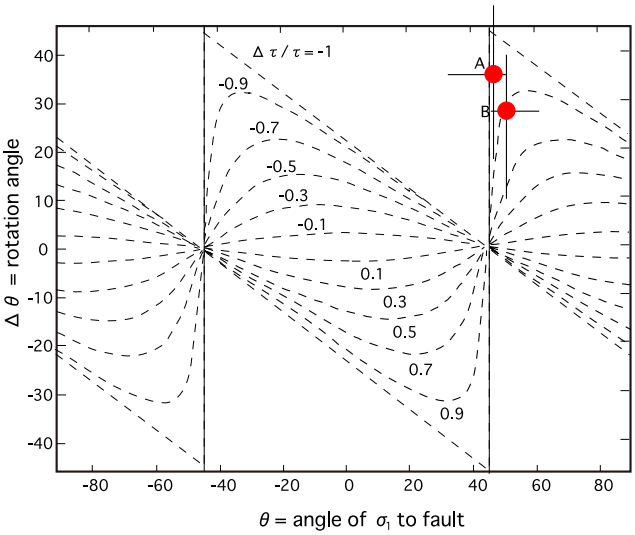

Fig. 6. Rotation of σ_1 axis ($\Delta\theta$) as a function of angle of σ_1 axis to the fault plane (θ) for various values of $\Delta\tau/\tau$, the ratio of stress drop to the deviatoric stress (Hardebeck and Hauksson, 2001). Presently estimated rotation angles for regions A and B are plotted by solid circles with the confidence ranges.

about 80 degrees. In Fig. 1(b), the intersecting angles of P-axes of some events at distances less than 200 km are not as large as 80 degrees. This is because the dip angle of the plate interface is shallow there and because the area in Fig. 1 is only a portion of the region B. Anyway, the 30–35 degree rotation of σ_1 axis due to the Tohoku earthquake is seen both for regions A and B.

4. Stress Magnitude, Fault Strength and Pore Pressure Ratio

Hardebeck and Hauksson (2001) obtained a general two-dimensional solution for the relationship between the near-field rotation of the stress field and the ratio of the earthquake stress drop $\Delta\tau$ to the background deviatoric stress magnitude τ. To obtain the solution, they assumed that the stress orientation is that observed at locations very near to the mainshock rupture, where the stress change can be approximated by the mainshock stress drop. As they discussed, this is a reasonable assumption for most aftershock sequences, since the majority of aftershocks occur along the mainshock rupture. In many cases, slip amount by the mainshock is not uniform in space but somewhat heterogeneous, which probably causes heterogeneity in stress and stress drop near the mainshock fault. However, if we assume that the observations are those which represent the uniform part of the stress field over the length scale of the mainshock rupture and stress drop is the average stress drop, then the average deviatoric stress on the mainshock fault can be obtained on the same length scale. Based on these assumptions, Hardebeck and Hauksson (2001) obtained a two-dimensional solution that relates the rotation angle of σ_1 axis with the mainshock stress drop, which shows that the rotation angle $\Delta\theta$ depends on only two parameters: θ, the orientation of the mainshock fault plane relative to the pre-mainshock σ_1 axis, and $\Delta\tau/\tau$, the ratio of the mainshock stress drop to the background deviatoric stress (Fig. 5). This relation allows us to estimate the ratio $\Delta\tau/\tau$ from observed θ and $\Delta\theta$. Hardebeck and Hauksson (2001) estimated $\Delta\tau/\tau$ to be $\sim$0.65 from the observed 15 degree rotation of σ_1 axis due to the 1992 M 7.3 Landers earthquake. They further estimated the deviatoric stress magnitude to be $\sim$12 MPa by using estimated average stress drop of $\sim$8 MPa.

Table 1. Estimated rotation angle, ratio of stress drop to background deviatoric stress, fault strength and pore pressure ratio.

Region	θ	$\Delta\theta$	$\Delta\tau/\tau$	τ	λ
A (N part of source area)	45°(32.5°–47°)	35°(17.5°–50°)	0.95(0.9–1.0)	21(20–22) MPa	94(94–95)%
B (S part of source area)	50°(45°–62.5°)	27.5°(10°–40°)	0.9(0.45–1.0)	22(20–44) MPa	94(88–95)%

Following Hardebeck and Hauksson (2001), we try to estimate the ratio $\Delta\tau/\tau$ from the observed rotation of the stress field. Figure 6 shows $\Delta\theta$ as a function of θ for various values of $\Delta\tau/\tau$ based on the solution by Hardebeck and Hauksson (2001). Presently observed $\Delta\theta$ and θ are plotted on the figure by red circles. Observed $\Delta\theta$ and θ for regions A and B fit with a curve of $\Delta\tau/\tau = 0.9$ or 0.95. This indicates that the background deviatoric stress was released nearly completely by the mainshock. Estimated $\Delta\tau/\tau$ and the range of its acceptable values are given in Table 1.

The average stress drop estimated from a slip model of the 2011 Tohoku earthquake based on GPS data is about 20 MPa (Iinuma *et al.*, 2011). Adopting this value as the mainshock stress drop $\Delta\tau$, the deviatoric stress magnitude τ can be estimated to be ∼21–22 MPa. This is nearly one order of magnitude less than the strength predicted by laboratory experiments for 10–50 km depths of the mainshock fault plane, suggesting that the plate interface in this depth range is weak.

Three types of models have been proposed for such weak faults (Hardebeck and Hauksson, 2001): existence of overpressured fluids on the fault (Rice, 1992; Sibson, 1992); existence of weak fault zone materials, although most of the candidate minerals tested by laboratory measurements were excluded (Morrow *et al.*, 1992; Moore *et al.*, 1996); and dynamic weakening of faults (Heaton, 1990). Presence of elevated pore-fluid pressure along the shallow plate boundary zone is most likely, since the oceanic plate contains abundant volume of aqueous fluids in its uppermost sedimental layer and the crust before its subduction.

If we assume the weak fault is caused by the overpressured fluids, then pore pressure ratio $\lambda = P_f/\sigma_n$ on the plate interface can be estimated from the Coulomb failure criterion $\tau = c + \mu(1-\lambda)\sigma_n$, where τ is shear stress, c cohesion, μ friction coefficient, σ_n normal stress and P_f pore fluid pressure. Adopting $c = 0$, $\mu = 0.6$ and $\sigma_n = 610$ MPa which is the lithostatic pressure at the average depth of the mainshock fault plane, we obtain $\lambda = \sim 0.94$. Estimated value and acceptable range of λ for regions A and B are given in Table 1. Average values of pore pressure ratio on the plate interface in several subduction zones in the world were estimated by Seno (2009) from the force balance between shear stress at the plate interface and the lithostatic pressure in the forearc wedge. The results show $\lambda = \sim 0.95$–0.98 for the plate boundary east off Tohoku, which is almost consistent with our estimation.

5. Discussion

As shown in Figs. 3(b) and (d), the dip angle of σ_1 axis became as high as 57.5–60 degrees after the Tohoku earthquake both for regions A and B. This high dip angle of σ_1 axis indicates that the original stress field of the thrust-fault type near the plate interface changed to that rather close to normal-fault type due to the occurrence of the Tohoku earthquake. Not only low-angle thrust-fault type aftershocks similar to the mainshock focal mechanism but also a significant number of normal-fault type aftershocks occurred in the case of the Tohoku earthquake (e.g., Asano *et al.*, 2011; Hirose *et al.*, 2011). This is caused by the nearly complete stress drop in the Tohoku earthquake demonstrated by the present study.

In Section 3, we assumed that the average dip angle of the plate interface is 20 degrees, since it varies from about 10 to 30 degrees. We further assumed that the stress field is uniform in the whole area of region A and that of region B, both of which include both the shallower and deeper portions of the main thrust zone with shallow and steep plate dips, respectively. This is because we attempted to extract information on a change of the average stress field for a wide area such as region A or region B, and the lateral variation of the stress change in the focal area of the mainshock, which perhaps exists, is beyond the scope of the present study.

The stress field in such a wide area as region A or B may not be sufficiently uniform. For example, the stress field around the edge of the mainshock fault plane possibly becomes heterogeneous to some extent. Actually, it seems that focal mechanisms of events in the Pacific plate at a distance of about 150 km in Fig. 1(b) show some scatters of P-axis directions. More detailed investigations including the lateral variations of the stress field are left for future studies.

6. Conclusions

We estimated the stress field near the fault plane of the 2011 Tohoku earthquake by inverting focal mechanisms of earthquakes. Comparison of the estimated stress fields before and after the earthquake shows a rotation of σ_1 axis after the mainshock. The σ_1 axis intersects with the plate interface at an angle of 45–50 degrees before the earthquake. This angle became to ∼80 degrees after the earthquake. The ratio of the mainshock stress drop to the background deviatoric stress $\Delta\tau/\tau$ was estimated to be 0.9–0.95 from the observed 30–35 degree rotation of σ_1 axis. Adopting the average stress drop of ∼20 MPa estimated from GPS data, we obtain the background deviatoric stress magnitude to be ∼21–22 MPa. The present observations indicate that the background deviatoric stress which caused the 2011 earthquake is mostly released, and that the deviatoric stress magnitude is low, of the order of a few tens of MPa, suggesting that the plate interface is weak. Assuming that this weak fault is caused by overpressured fluids, pore pressure ratio on the plate interface is estimated to be ∼0.94.

Acknowledgments. We used focal mechanism data from the F-net seismic moment tensor catalogue provided by the National Research Institute for Earth Science and Disaster Prevention.

Thoughtful comments from Y. Iio and G. Ekstrom significantly improved the manuscript. This work was supported in part by the Global COE Program, "Global Education and Research Center for Earth and Planetary Dynamics" at Tohoku University, and the Scientific Research Program on Innovative Areas, the "Geofluids: Nature and Dynamics of Fluids in Subduction Zones" at Tokyo Institute of Technology.

References

Asano, Y., T. Saito, Y. Ito, K. Shiomi, H. Hirose, T. Matsumoto, S. Aoi, S. Hori, and S. Sekiguchi, Spatial distribution and focal mechanisms of aftershocks of the 2011 off the Pacific coast of Tohoku Earthquake, *Earth Planets Space*, **63**, this issue, 669–673, 2011.

Gephart, J. W. and D. W. Forsyth, An improved method for determining the regional stress tensor using earthquake focal mechanisms data: Application to the San Fernando earthquake sequence, *J. Geophys. Res.*, **89**, 9305–9320, doi:10.1029/JB089iB11p09305, 1984.

Hardebeck, J. and E. Hauksson, Crustal stress field in southern California and its implications for fault mechanics, *J. Geophys. Res.*, **106**(B10), 21859–21882, 2001.

Heaton, T. H., Evidence for and implications of self-healing pulses of slip in earthquake rupture, *Phys. Earth Planet. Inter.*, **6**, 1–20, 1990.

Hirose, F., K. Miyaoka, N. Hayashimoto, T. Yamazaki, and M. Nakamura, Outline of the 2011 off the Pacific coast of Tohoku Earthquake (M_w 9.0)—Seismicity: foreshocks, mainshock, aftershocks, and induced activity—, *Earth Planets Space*, **63**, this issue, 513–518, 2011.

Iinuma, T., M. Ohzono, Y. Ohta, and S. Miura, Coseismic slip distribution of the 2011 off the Pacific coast of Tohoku Earthquake (*M* 9.0) estimated based on GPS data—Was the asperity in Miyagi-oki ruptured?, *Earth Planets Space*, **63**, this issue, 643–648, 2011.

Ito, Y., Y. Asano, and K. Obara, Very-low-frequency earthquakes indicate a transpressional stress regime in the Nankai accretionary prism, *Geophys. Res. Lett.*, **36**, L20309, doi:10.1029/2009GL039332, 2009.

Moore, D. E., D. A. Lockner, R. Summers, S. Ma, and J. D. Byerlee, Strength of chrysotile-serpentinite gouge under hydrothermal conditions: Can it explain a weak San Andreas Fault?, *Geology*, **24**, 1041–1044, 1996.

Morrow, C., B. Radney, and J. Byerlee, Frictional strength and the effective pressure law of montmorillonite and illite clays, in *Fault Mechanics and Transport Properties of Rock*, edited by B. Evans and T.-F. Wong, pp. 69–88, Academic, San Diego, Calif., 1992.

Nakajima, J., F. Hirose, and A. Hasegawa, Seismotectonics beneath the Tokyo metropolitan area: Effect of slab-slab contact and overlap on seismicity, *J. Geophys. Res.*, **114**, B08309, doi:10.1029/2008JB006101, 2009.

Rice, J. R., Fault stress states, pore pressure distributions, and the weakness of the San Andreas Fault, in *Fault Mechanics and Transport Properties of Rock*, edited by B. Evans and T.-F. Wong, pp. 475–503, Academic, San Diego, Calif., 1992.

Seno, T., Determination of the pore fluid pressure ratio at seismogenic megathrusts in subduction zones: Implications for strength of asperities and Andean—type mountain building, *J. Geophys. Res.*, **114**, B05405, doi:10.1029/2008JB005889, 2009.

Sibson, R. H., Implications of fault-valve behaviour for rupture nucleationa nd recurrence, *Tectonophysics*, **211**, 283–293, 1992.

Umino, N., A. Hasegawa, and T. Matsuzawa, sP depth phase at small epicentral distances and estimated subducting plate boundary, *Geophys. J. Int.*, **120**, 356–366, 1995.

A. Hasegawa (e-mail: hasegawa@aob.geophys.tohoku.ac.jp), K. Yoshida, and T. Okada